Fabrication and characterization of a TiO_2/polysiloxane resin composite coating with full-thickness super-hydrophobicity

Chunling Li, Yangchao Sun, Meng Cheng, Shuangqing Sun, Songqing Hu

PII: S1385-8947(17)31664-9
DOI: https://doi.org/10.1016/j.cej.2017.09.165
Reference: CEJ 17750

To appear in: *Chemical Engineering Journal*

Received Date: 18 April 2017
Revised Date: 9 August 2017
Accepted Date: 25 September 2017

Please cite this article as: C. Li, Y. Sun, M. Cheng, S. Sun, S. Hu, Fabrication and characterization of a TiO_2/polysiloxane resin composite coating with full-thickness super-hydrophobicity, *Chemical Engineering Journal* (2017), doi: https://doi.org/10.1016/j.cej.2017.09.165

Fabrication and characterization of a TiO_2/polysiloxane resin composite coating with full-thickness super-hydrophobicity

Chunling Li[a,b], Yangchao Sun[a], Meng Cheng[a], Shuangqing Sun[a,b,*], Songqing Hu[a,b,*]

[a] *College of Science, China University of Petroleum (East China), Qingdao 266580, China*

[b] *Key Laboratory of New Energy Physics & Materials Science in Universities of Shandong (China University of Petroleum (East China)), Qingdao 266580, China*

Abstract

We present a simple approach for the fabrication of a full-thickness super-hydrophobic composite coating consisted of modified TiO_2 nanoparticles and polysiloxane resin. Scanning electron microscope (SEM), fourier transform infrared spectrometer (FTIR), contact angle meter and a simple self-made device were employed to characterize the surface morphologies, chemical compositions, contact angle and sliding angle of the modified TiO_2 nanoparticles and composite coating, respectively. Results show that for both the modified TiO_2 nanoparticles and the as-prepared composite coating the contact angle and sliding angle of is up to 152° and 0°, respectively. In addition, due to the coating design of full-thickness super-hydrophobicity, the composite coating also exhibited good thermal stability, abrasion resistance and corrosion resistance in the thermo-gravimetric analysis (TGA) experiment, abrasion test and immersion test, respectively.

Keywords: super-hydrophobic, TiO_2, polysiloxane resin, corrosion resistance, abrasion resistance

1 Introduction

Super-hydrophobic surfaces with a water contact angle (CA) higher than 150° and a sliding angle (SA) lower than 10° have attracted much attention due to their wide range of applications such as oil/water separation[1, 2], anti-corrosion[3, 4], fluid drag reduction[5, 6], anti-icing[3, 6], self-cleaning[3, 7] and transparent coating[8, 9], etc. According to previously reported studies, there are two keys to fabricate super-hydrophobic surfaces, i.e. appropriate surface features (to trap air) and low surface free energy (to repel water). Researchers have explored a series of approaches to prepare super-hydrophobic surfaces based on the above two key factors, including template method[10], sol-gel method[11], vapor deposition method[12], chemical etching[13], and electrospinning method[14], etc. However, most methods need expensive raw materials, special equipments, or multistep procedures. In addition, most super-hydrophobic surfaces easily lose the super-hydrophobicity once the micro/nanostructures of coatings are mechanically damaged, which seriously limits their practical applications and shortens their lifetime.

Recently, nanoscale materials have been extensively applied in the preparation of the super-hydrophobic surface due to their special physical and chemical properties, such as excellent hardness, optimal micro/nanostructure and high specific surface area, etc. However, the super-hydrophobic coating, fabricated by only nanoparticles, has a bad durability because of its poor adhesion among nanoparticles and that between nanoparticles and substrate. Therefore, some preparation processes of super-hydrophobic coating combining the usage of nanoparticles and polymers have

been proposed. Nanoparticles, such as SiO_2[15], TiO_2[16], Al_2O_3[17], ZnO[18], C[19] and $CaCO_3$[20] are frequently used for fabricating super-hydrophobic coating. Qing et al.[21] have prepared a modified-TiO_2/polyvinylidene fluoride composite surface on the Cu substrate via a dip-coating process, with a contact angle of 160.1° and a sliding angle of 5.5°, which shows good corrosion resistance and reversible superhydrophobicity/superhydrophilicity. Hancer et al.[22] have achieved polymer thin film nanocomposites by dispersing modified-SiO_2 into a poly silicon (silsesquioxane) matrix, with a contact angle of 178°, which exhibits good wear-resisting performance and anti-icing property. Wang at al.[23] have prepared a PTFE nanoparticles-filled coating surfaces with a contact angle of 163°, which has a good thermal stability and acid resistance. However, most researchers used polymer or resin as the matrix of the coating and nanoparticles as additive dispersed in the matrix. These coatings, especially those with a high content of resin, are susceptible to failure such as coating blister and cracking once the corrosive medium penetrates the coating. Recently a new coating system named "substrate/glue/superhydrophobic nanoparticles" was proposed. In this coating system, the glue (adhesive or polymer) bonds the superhydrophobic nanoparticles onto the substrate strongly. Lu et al.[24] have prepared robust self-cleaning surfaces by spraying the ethanolic suspension of perfluorosilane-coated TiO_2 nanoparticles onto the substrates coated with commercial adhesives, and the prepared coating shows great robustness. Chen et al.[25] prepared a "glass/glue/modified-$CaCO_3$" coating system which has a good robustness and oil-water separation performance. Zhang et al [26] have prepared a porous

superhydrophobic and superoleophilic surface using template assisted chemical vapor deposition (CVD) for oil/water separation. The prepared surface shows good mechanical robustness, high chemical resistance and high recyclability. This type of coating system was easily prepared and had superior abrasion resistance. However, the corrosion resistance of this coating system was poor when it was immersed into the corrosive medium and the corrosion ion penetrated the thin nano-coating easily (according to the immersion test).

In this context, we proposed a new coating system in which the functionalized TiO_2 nanoparticles were used as the body of composite coating, while a small amount of polysiloxane resin was used as the binder to bond the nanoparticles together and improve the adhesion of the whole composite coating to the substrate. The corrosion resistance and wear resistance of the coating were emphatically studied and some interesting results were obtained. As far as we know, it is the first time that the coating system presented in this work was proposed. Based on the characterization and properties testing results, the proposed coating system in this work was found to have good thermal stability, abrasion resistance and corrosion resistance due to the super-hydrophobicity in the full thickness of the coating.

2 Experimental methods

2.1 Modification of TiO_2 nanoparticles

Rutile TiO_2 nanoparticles with a diameter of 25 nm and a contact angle of 0° (purchased from Shanghai Aladdin-Reagent Co., Ltd) were modified by a simple hydrothermal reaction in order to obtain the superhydrophobicity. In the modification

process of TiO_2 nanoparticles, 0.5 g triethoxyoctylsilane was dissolved into 50 ml ethanol firstly and stirred for 2 h under 60 °C to make the triethoxyoctylsilane fully hydrolyzed in the ethanol to obtain solution A. Then, 3 g rutile TiO_2 nanoparticles were added into the solution A and continuously stirred for another 3 h to form the suspension B. Finally, the obtained suspension B was dried at 120 °C for 2 h to achieve super-hydrophobic TiO_2 nanoparticles. The preparation of super-hydrophobic TiO_2 nanoparticles is shown in Figure 1. The possible mechanism for the formation of super-hydrophobic TiO_2 nanoparticles is shown in Figure 2.

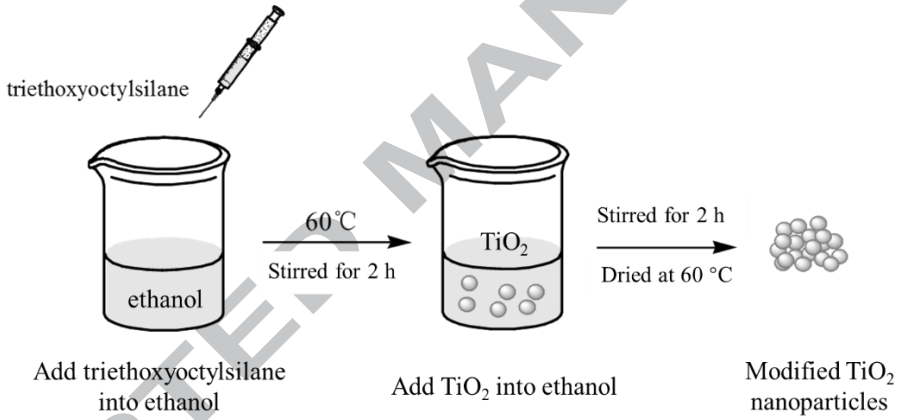

Figure 1. Schematic illustration for the preparation of super-hydrophobic TiO_2 nanoparticles

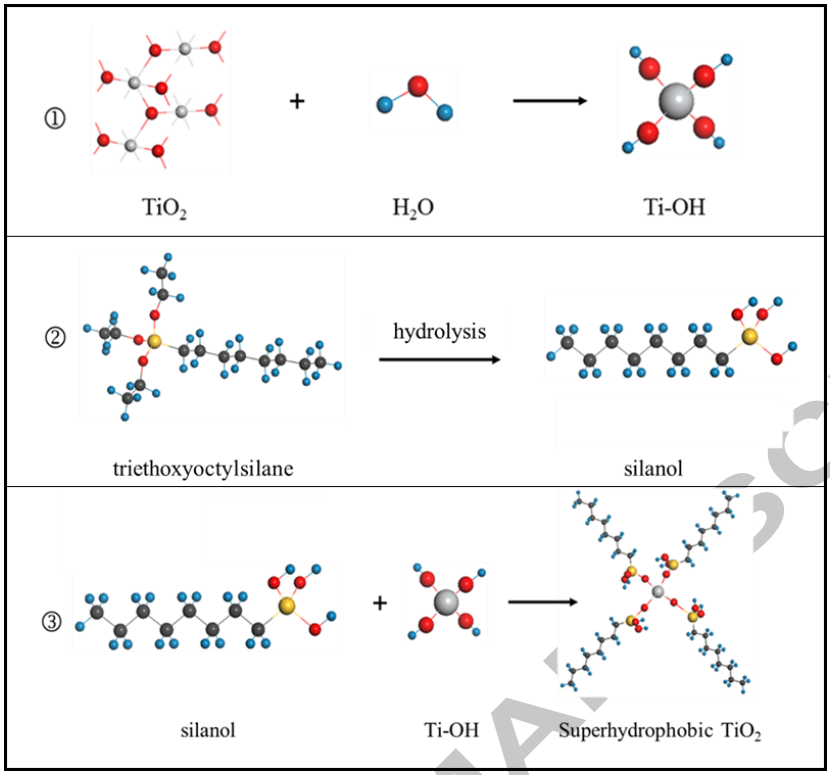

Figure 2. Possible mechanism for the formation of super-hydrophobic TiO_2 nanoparticles formation (●:O; ●:C; ●:Ti; ●:Si; ●:H). ①, ② and ③ indicates step 1 (Surface hydroxylation of R-SiO_2), step 2 (Hydrolysis of triethoxyoctylsilane), and step 3 (Hydrophobization of TiO_2 nanoparticles) for the formation of super-hydrophobic TiO_2 nanoparticles, respectively.

2.2 Preparation of super-hydrophobic TiO_2/polysiloxane resin composite coating

In this work, super-hydrophobic TiO_2/polysiloxane resin composite coating was prepared by mixing the previously prepared super-hydrophobic TiO_2 nanoparticles and polysiloxane resin which is composed of 60% polysiloxane and 40% propylene glycol methyl ether. The structural formula and fourier transform infrared (FTIR) spectrum of this polysiloxane resin are shown in Figure 3. The band at 2970 cm^{-1}, 2880 cm^{-1} and 2925 cm^{-1} are due to the stretching vibration of $–CH_3$ and $–CH_2$. The band at 1100 cm^{-1}, 800 cm^{-1} are due to the stretching vibration of Si-O and C-Si. The existence of these bands indicates that the resin we used in the composite coating is a

polysiloxane system, and the FTIR result is consisted with the molecular formula. In the structural formula, the R is on behalf of benzene ring, carbamido and so on. The degree of polymerization *n* is about 100. Firstly, 3 g super-hydrophobic TiO_2 nanoparticles (prepared in Section 2.1) were added into 15 mL propylene glycol monomethyl ether under the ultrasonic dispersion for 5 min, and then the polysiloxane resin was added proportionally into the TiO_2 solutions. In this work, in order to investigate the effect of the polysiloxane resin content on the superhydrophobicity of composite coating, the additive amount of polysiloxane resin for 3 g super-hydrophobic TiO_2 nanoparticles was 0.5, 1, 1.5 and 2 g. The mixture of polysiloxane resin and super-hydrophobic TiO_2 nanoparticles was continuously stirred for 1 h at 50 °C to obtain a uniform suspension. Secondly, the prepared suspension was manually brushed onto the carbon steel plate with a size of 50×50×2 mm to form the composite coating. In this work, the carbon steel substrates were pretreated using a sand blast machine and ultrasonically degreased in acetone before brushing the coating. Finally, the coating samples were placed in a drying oven at 40 °C for 12 h to promote the volatilization of solvent and the curing of resin. In the formation of coating, the TiO_2 nanoparticles do not react with polysiloxane resin. In this work, the thickness of the as prepared coating is about 80 μm (detected using a Elcometer 456 coating thickness gauge). The schematic diagram of the composite coating structure is shown in Figure 4.

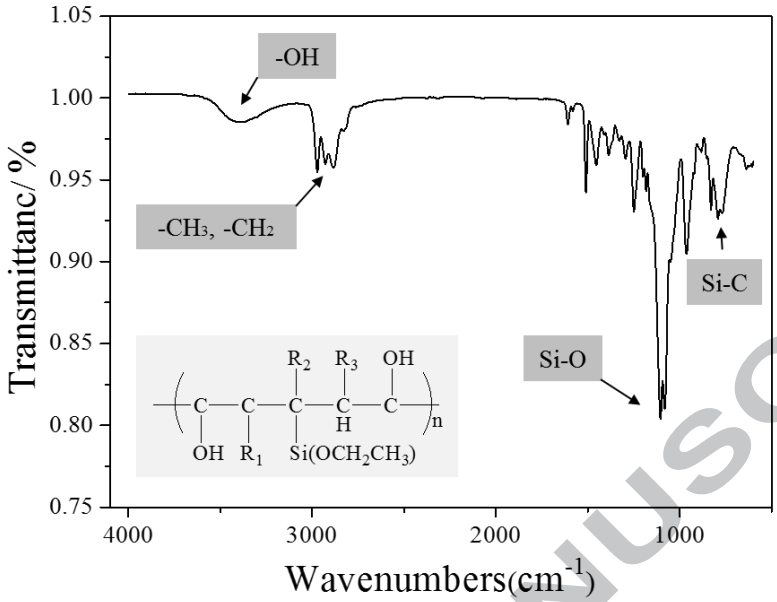

Figure 3. Structural formula and FTIR spectrum of polysiloxane resin

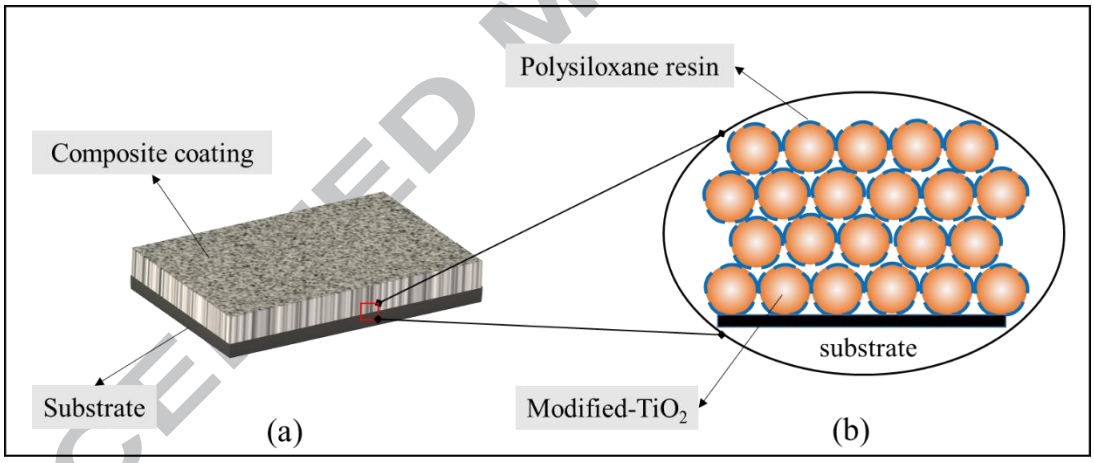

Figure 4. Schematic diagram of structure of the composite coating.

2.3 Characterization of modified TiO_2 nanoparticles and TiO_2/polysiloxane resin composite coating

2.3.1 Microstructure , chemical composition and surface energy test

The microstructure of the composite coating was observed by scanning electron microscope (SEM, S-4800, Hitachi). The chemical composition of modified TiO_2 nanoparticles and composite coating was analyzed by fourier transform infrared

spectrometer (FTIR, nicolet-6700, Thermo Fisher). Meanwhile, the surface energy of the initial TiO_2 nanoparticles and super-hydrophobic TiO_2 nanoparticles was detected by a contact angle meter (JC-2000, Zhong Chen, Shang Hai). The detection method is based on the "Owens two fluid method"[27].

2.3.2 Contact angle (CA), sliding angle (SA) measurements and bouncing test

In order to evaluate the hydrophobicity of modified TiO_2 nanoparticles, some suspension B (prepared in section 2.1) was directly sprayed onto the glass slide and dried in a drying oven. After drying, we obtained a coating consisted of pure modified TiO_2 nanoparticles. Then, a contact angle meter (JC-2000, Zhongyi) was used to measure the contact angle (CA) of pure modified TiO_2 coating at room temperature. CA values were the averages of at least five measurements performed at different positions with 3 μL water droplets. For the TiO_2/polysiloxane resin composite coating, CA measurements were directly performed on the coating surface with the same method as described above.

The sliding angle (SA) of the modified TiO_2 nanoparticles and TiO_2/polysiloxane resin composite coatings was measured by a simple self-made device shown in Figure 5. In the SA measurements, the one side of the coating sample was fixed, and the other side was placed on the glass slide. The tilted angle α of samples, i.e., the sliding angle of water droplet (12 μL) on the samples, could be determined by increasing the number of slides till the water droplet starts to slide. The sliding angle α could be calculated by the equation below.

$$\alpha = \arctan (H/L) \quad (1)$$

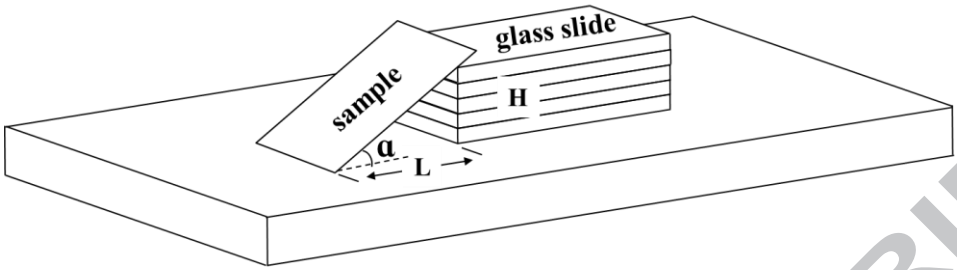

Figure 5. Schematic diagram of the device used to measure the sliding angle

The water bouncing test was carried out by the same contact angle meter as used for SA and CA measurements. Briefly, the process of water droplets dropping from syringe and bouncing from composite coatings was recorded through the contact angle meter.

2.4 Thermal stability test of TiO_2 nanoparticles and TiO_2/polysiloxane resin composite coatings

In this work, in order to study the effect of temperature on the weight of composite coating, thermogravimetric analysis (TGA) experiments were performed on the TiO_2/polysiloxane resin composite coating and pure polysiloxane resin as well as TiO_2 nanoparticles (before and after modification) through a METTLER STAR system (TGA/DSC1, Mettle) at a heating rate of 10 °C/min under pure oxygen atmosphere.

In particular, the effect of temperature on the hydrophobicity of the TiO_2/polysiloxane resin composite coatings was also studied by putting the sample into a drying oven under a series of different temperatures (60, 80, 100, 120, 140, 160 °C) for 24 h. CA and SA of composite coatings were measured after drying with the same methods as described in section 2.3.2.

2.5 Abrasion test of TiO_2/polysiloxane resin composite coatings

The abrasion resistance of the TiO_2/polysiloxane resin composite coating was evaluated by sandpaper abrasion test. The schematic diagram of testing apparatus is shown in Figure 6. The testing apparatus mainly consists of a weight of 250 g and a 180 grit sandpaper with the size of 28 cm in length and 20 cm in width. Firstly, the composite coating was positioned facing to sandpaper, and the weight of 250 g was put on the composite coating. Secondly, the sample was moved for 20 cm in one direction, then the sample was rotated by 90° (coating side still faced to the sandpaper) and moved for another 20 cm in the opposite direction. This whole process described above was defined as one abrasion cycle. Before and after abrasion test, the weight of coating sample was measured and the weight change was calculated. In addition, CA and SA of composite coatings were also measured with the same methods as described in section 2.3.2 before and after abrasion test. The abrasion resistance was evaluated by both weight change and CA/SA change.

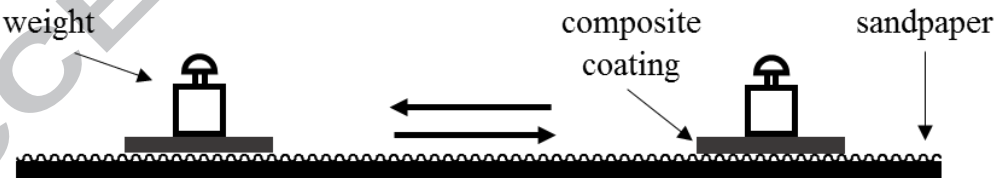

Figure 6. Schematic diagram of sandpaper abrasion test

2.6 Corrosion test of TiO_2/polysiloxane resin composite coatings

In this work, corrosion resistance of composite coatings was investigated by immersion test in 3.5 wt % NaCl solution. In the immersion test, the hydrophobicity change of composite coatings subjected to immersion test for different lengths of time was studied through measuring CA of the samples. In addition, corrosion morphology

of immersed samples was also observed periodically in order to evaluate the protectiveness for the carbon steel substrate. As a reference, the corrosion morphologies of pure epoxy resin coating and pure polysiloxane resin coating without the addition of TiO_2 nanoparticles were also observed. For the convenience of measurement, the back face and side faces of the samples were sealed by paraffin.

3 Results and discussion

3.1 Characterization of modified TiO_2 nanoparticles and TiO_2/polysiloxane resin composite coatings

3.1.1 Microstructure

SEM images of TiO_2 particles (25 nm in the diameter) before and after modification are shown in Figure 7. Overall, TiO_2 nanoparticles do not exhibit apparent change after modification in appearance. Also it can be seen that agglomeration occurs on nanoparticles both before and after modification, forming bigger spheres (~100 nm in diameter) with a rough hierarchical structure. However, there are a great number of voids among these bigger spheres, i.e., agglomerated nanoparticles. Both the rough hierarchical structure of agglomerated nanoparticles and voids among them are beneficial for the surface to trap air and repel water, which lays the foundation for the fabrication of super-hydrophobic composite coatings.

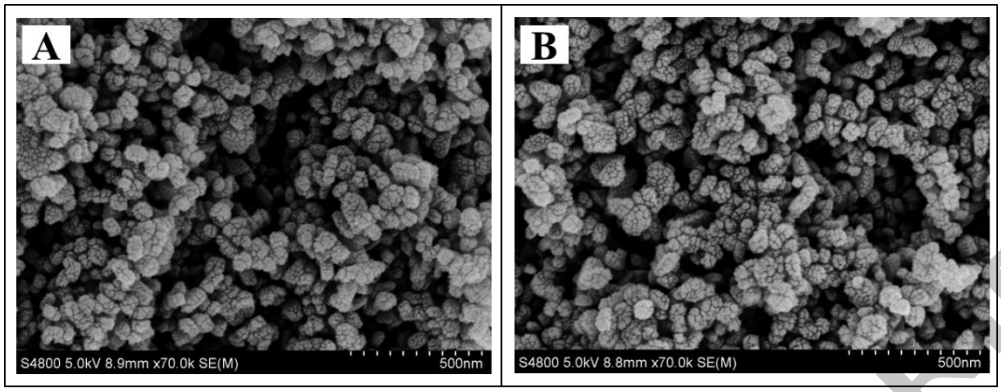

Figure 7. SEM images of TiO_2 raw material (a) and modified-TiO_2 nanoparticles (b)

Figure 8 shows the surface morphologies of TiO_2/polysiloxane resin composite coatings. The surface of the composite coating is very rough according to Figure 8a. Compared with the pure TiO_2 nanoparticles, the SEM image of the as-prepared super-hydrophobic composite coating surface shows that more obvious agglomeration occurs when the polysiloxane resin was added into TiO_2 nanoparticles to form composite coating (Figure 8b). In the composite coating, TiO_2 nanoparticles agglomerate to bigger particles with a wide range of diameter from ~ 20 to ~ 200 μm. However, these further agglomerated particles can still exhibit a very loose and porous surface.

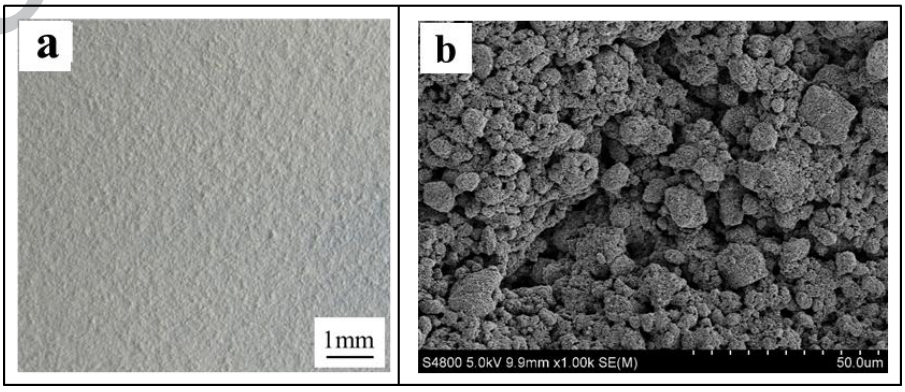

Figure 8. Macrograph (a) and SEM (b) of TiO_2/polysiloxane resin composite coating surface

3.1.2 Chemical composition

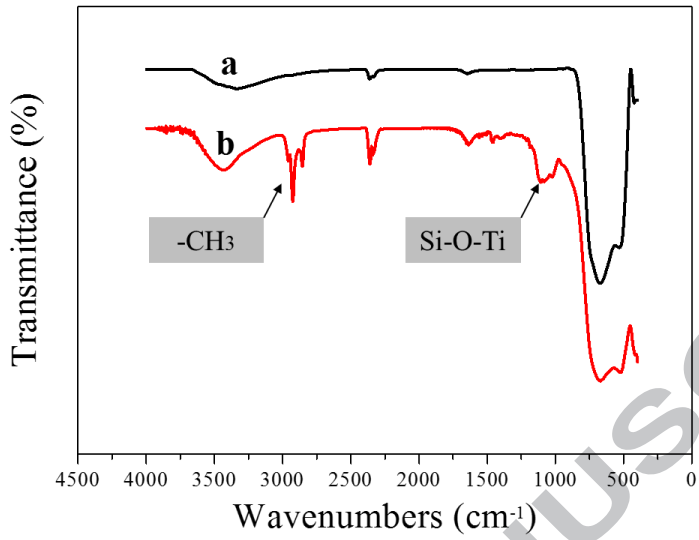

Figure 9a and Figure 9b show the FTIR spectra of the TiO_2 nanoparticles before and after modification, respectively. Compared with the raw TiO_2 nanoparticles, there are some new peaks in the spectrum of modified TiO_2 nanoparticles. The peak at 1072 cm^{-1} is thought to be attributed to the asymmetric stretching vibration of the Si-O-Ti species, and the peak at 2925 cm^{-1} and 2857 cm^{-1} is attributed to the symmetric stretching vibration and the asymmetric stretching vibration of $-CH_2$ groups, respectively. The absorption peaks at about 2954 cm^{-1} and 1460 cm^{-1} are due to the asymmetric stretching vibration and the asymmetric bending vibration of $-CH_3$. The existence of these peaks proves the occurrence of dehydration reaction between hydrolytic triethoxyoctylsilane molecules and TiO_2 nanoparticles, which confirms the success of modification process. Figure 9b also shows that the super-hydrophobic TiO_2 nanoparticles have more hydroxyl groups (the band at 3424 cm^{-1} represents -OH) compared with the spectrum of TiO_2 raw material (Figure 9a). This might be caused by excessive silanol groups which did not react with the hydroxyls.

Figure 9. FTIR spectra of initial TiO_2 nanoparticles (a) and modified-TiO_2 nanoparticles (b).

The success of modification process can also be confirmed by the surface energy of the initial TiO_2 and superhydrophobic TiO_2 nanoparticles. From Table 1, it can be seen that the surface energy of the nanoparticles decreased from 72.4 to 19.1 $J \cdot m^{-2}$ after modification, which suggests that the initial TiO_2 nanoparticles were modified by triethoxyoctylsilane successfully.

Table 1 Surface energy of the initial TiO_2 nanoparticles, super-hydrophobic TiO_2 nanoparticles and TiO_2/polysiloxane resin composite coating

Sample	Surface energy ($J \cdot m^{-2}$)
polysiloxane resin	32.9
initial TiO_2 nanoparticles	72.4
super-hydrophobic TiO_2 nanoparticles	19.1
TiO_2/polysiloxane resin composite coating	17.8

3.1.3 Hydrophobicity

In the CA and SA measurements, the modified TiO_2 nanoparticles (prepared in Section 2.1) was found to have a contact angle of ~ 151° and a sliding angle of ~ 3°, indicating that the modified TiO_2 nanoparticles with the diameter of 25 nm have a good super-hydrophobicity. This is the foundation of the formation of super-hydrophobic composite coating. CA and SA of TiO_2/polysiloxane resin composite coatings with different polysiloxane resin content are shown in Figure 10. It can be seen that when the addition amount of polysiloxane resin is lower than 2 g for 3 g TiO_2 nanoparticles, the composite coatings have a good hydrophobicity with a

contact angle of 152° and a sliding angle close to 0°. However, the hydrophobicity of composite coatings is greatly declined when the additive amount of polysiloxane resin increases to 2 g, having a contact angle of 130° and a sliding angle of 69°. The decrease of hydrophobicity for the composite coating with the high content of polysiloxane resin is thought to be due to the excessive addition of polysiloxane resin with a high surface free energy. From Tbale 1, the surface energy of polysiloxane is 32.9 $J \cdot m^{-2}$ which is higher than modified nanoparticles (19.1 $J \cdot m^{-2}$) and composite coating (17.8 $J \cdot m^{-2}$). This not only increases the surface free energy of the composite coating, but also decreases the surface roughness of the composite coating owing to the insufficient exposure of super-hydrophobic TiO_2 nanoparticles on the coating surface. Though the composite coatings containing 0.5 g and 1 g polysiloxane resin also have a good hydrophobicity, their mechanical property (such as abrasion resistance, cohesion strength and bonding strength, etc.) is supposed to be poorer than the composite coating containing 1.5 g polysiloxane resin because of the low resin content. Therefore, in this work the composite coating with 1.5 g polysiloxane resin was used in the following characterization and tests of abrasion and corrosion resistance.

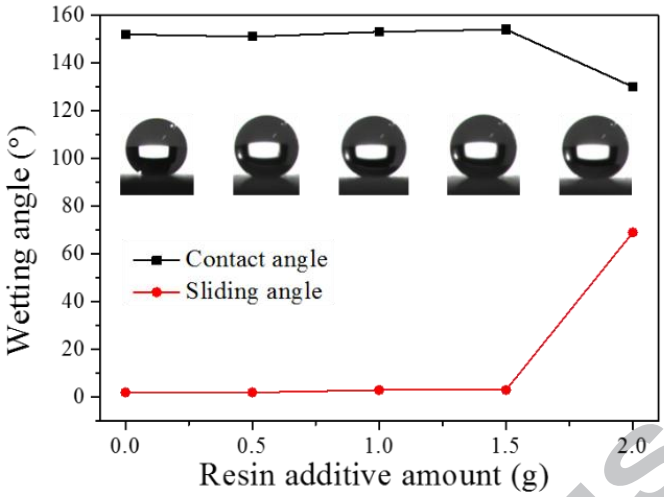

Figure 10. Contact angles and sliding angles of composite coatings with different resin content

The result of water bouncing test was shown in Figure 11. We can see that water droplets completely leave the surface without wetting or contaminating the surfaces (the water was dyed blue to aid visualization), indicating that the surfaces were super-hydrophobic.

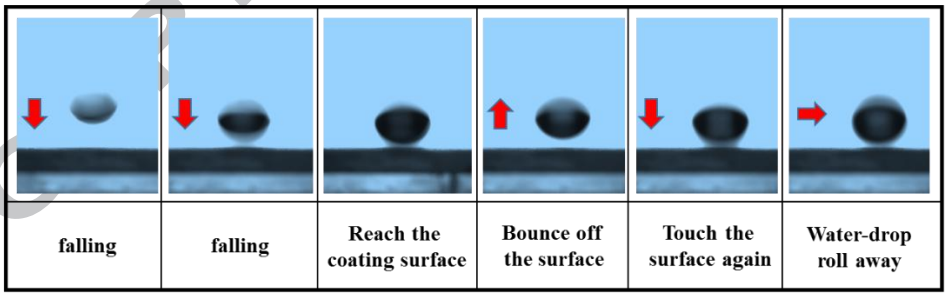

Figure 11 Process of water droplet bouncing on the composite coating.

3.2 Thermal stability of TiO_2/polysiloxane resin composite coating

3.2.1 Effect of temperature on the weight loss of composition coating

The TGA spectrum of the TiO_2/polysiloxane resin composite coating is shown in Figure 12, as well as that of pure polysiloxane resin, TiO_2 nanoparticles before and after modification. It can be seen that before and after modification the weight of TiO_2

nanoparticles does not exhibit apparent change over the whole temperature range from 40 °C to 900 °C, which indicates that TiO_2 nanoparticles have excellent thermal stability. However, with the increase of the temperature, the weight of composite coating shows a slight decrease when the temperature is below 300 °C. In particularly, the weight loss of composite coating is lower than 1% (0.9%) when the temperature is 160 °C. Therefore, it could be proposed that the effect of temperature on the composite coating is indistinctive when the temperature is below 160°C. Rapid weight loss of the composite coating occurs under the temperature range of 300−600 °C. When the temperature reaches 600 °C, the weight loss of composite coating is about 20%. The weight loss of composite coating is mainly caused by the decomposition of polysiloxane resin. From figure 12d, it can be seen that the weight loss of resins show obvious decrease in the whole temperature range. When the temperature reaches 600 °C, the weight loss of polysiloxane resin is higher than 80%.

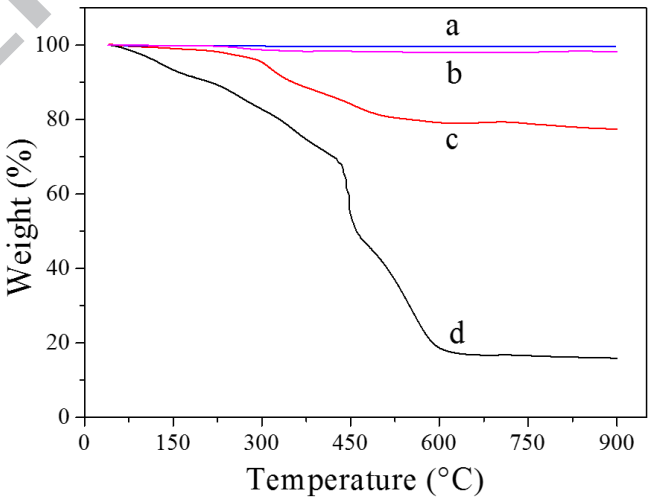

Figure 12. TGA spectrum of TiO_2 nanoparticles before modification (a), TiO_2 nanoparticles after modification (b), composite coating (c) and pure polysiloxane resin (d).

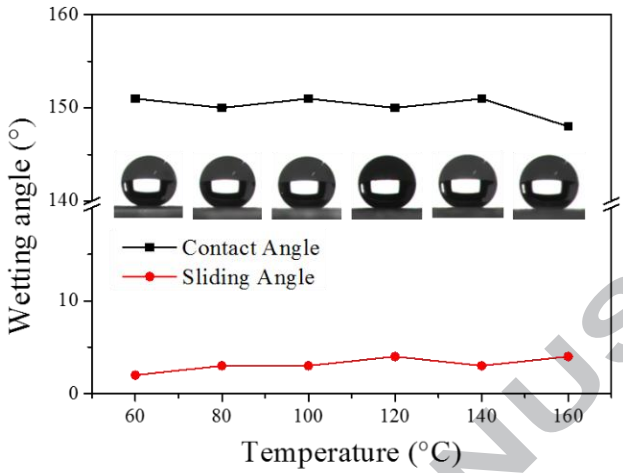

Figure 13. Contact angles and sliding angles of composite coatings after 24 h drying under different temperature

3.2.2 Effect of temperature on the hydrophobicity of composite coating

The effect of temperature on the hydrophobicity of the composite coating was also studied in this work. The temperature gradient was set as 60, 80, 100, 120, 140 and 160 °C. CA and SA of the composite coatings after 24 h drying under different temperature are shown in Figure 13. It can be seen that the composite coating had a stable contact angle of ~150° and sliding angle of ~3° over the temperature range of 60~160 °C. This indicates that the composite coating can keep its super-hydrophobicity when the temperature is under 160 °C. The thermal stability of composite coating is attributed to the superhydrophobic TiO_2 nanoparticles. The contact angles of the super-hydrophobic TiO_2 nanoparticles before and after thermogravimetry experiments were detected. From Figure 14, we can see that the

contact angle has little change after TGA test and the CA of TiO_2 nanoparticles is still 150°. The stable contact angle suggests that the high temperature has little influence on the super-hydrophobicity of the nanoparticles.

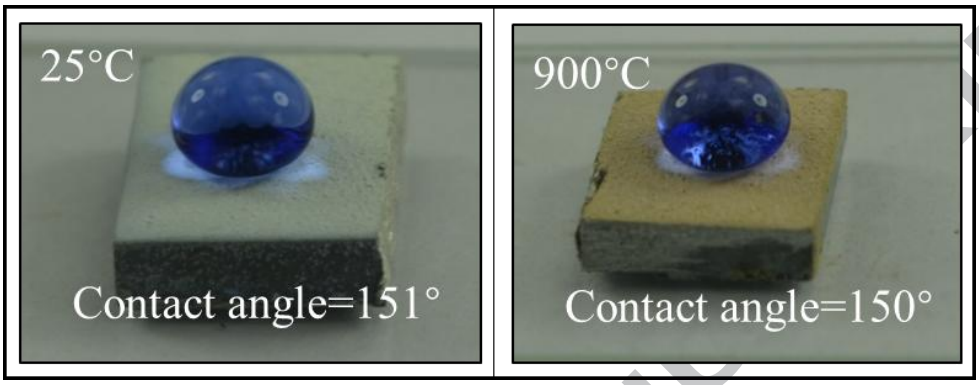

Figure 14. Contact angle of the super-hydrophobic TiO_2 nanoparticles before (25℃) and after (900℃) TGA test.

3.3 Abrasion resistance of TiO_2/polysiloxane resin composite coating

After abrasion test, the weight loss of the super-hydrophobic composite coating is about 0.0748 g (the initial weight is 38.4727 g, and the final weight is 38.3979 g). In contrast, the pure TiO_2 coating (prepared in section 2.3.2) without the addition of polysiloxane resin is easily erased even by finger wiping. This indicates that the cohesion strength between nanoparticles as well as the adhesion between composite coating and substrate was greatly improved by the addition of polysiloxane resin. Figure 15 shows the contact angles of super-hydrophobic composite coatings after abrasion tests with different abrasion cycles. It is clearly seen that the contact angle of the composite coating has little change even after 10-cycle sandpaper abrasion test. Figure 16 shows the surface morphology of the composite coating and the optical images of liquid drops on the coating surface after abrasion. There are some scratches on the surface showing that the surface layer of composite coatings has been worn

away (Figure 16a), but the "new surface" is still very rough (inset in Figure 16a). The "new surface" with a water contact angle of 151° still shows excellent hydrophobicity (Figure 16b), which indicates that the whole coating is super-hydrophobic not only on the surface of the coating but also inside the coating.

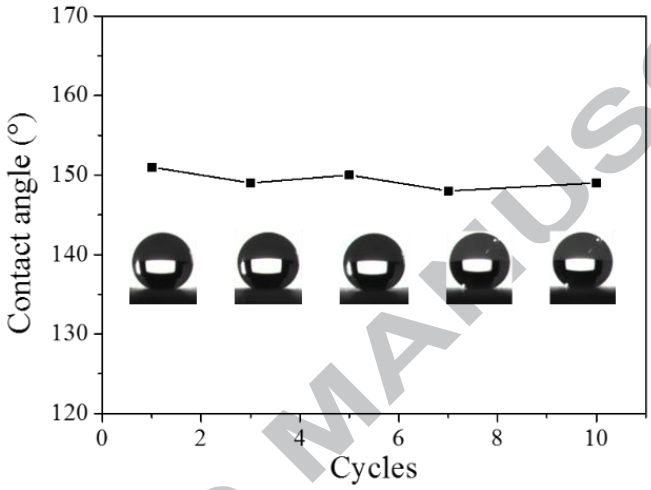

Figure 15. Water contact angles of composite coating after different cycles of abrasion testing

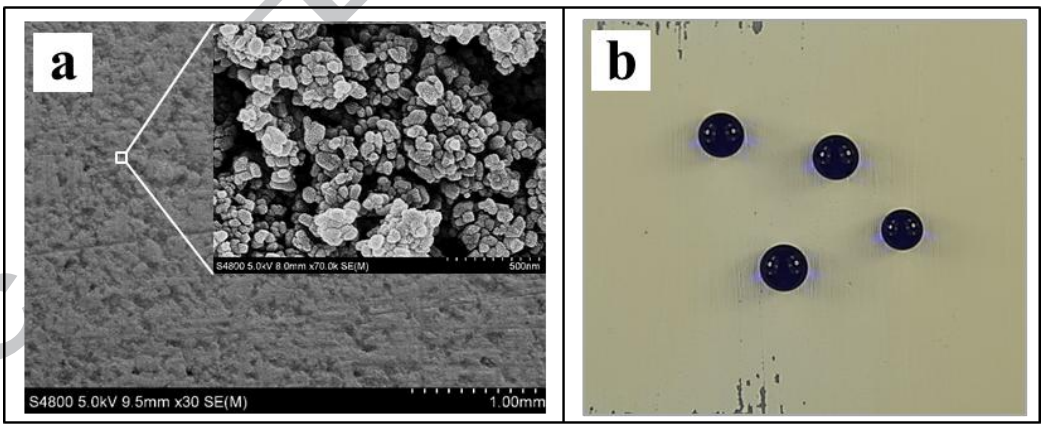

Figure 16. Surface morphology of the composite coating (a) and the optical image of liquid drops on the composite coating surface (b) after abrasion testing. Inset in Figure 14a is the SEM image showing the partial enlarged worn coating.

3.4 Corrosion resistance of TiO_2/polysiloxane resin composite coating

Figure 17 shows the corrosion morphologies of three kinds of coatings after

different immersion time, including super-hydrophobic composite coating, pure polysiloxane resin coating and pure epoxy resin coating. It should be noted that these coatings have the same carbon steel substrate. It is seen that pure polysiloxane resin coatings have cracked after immersion for 1 d, and there are many green corrosion spots on the surface of steel plate. This indicates that the sodium chloride solution has penetrated the polysiloxane resin coating and corroded the metal substrate. In addition, the corrosion is more and more serious with the increase of the immersion time, and the coating completely lose its protection ability for steel substrate after 6-day immersion. For the pure epoxy resin coating, some blisters appear on the surface of epoxy resin coatings after 16-day immersion, indicating that the sodium chloride solution has penetrated the coating. The super-hydrophobic TiO_2/polysiloxane resin composite coating, by contrast, has good corrosion protection performance in the

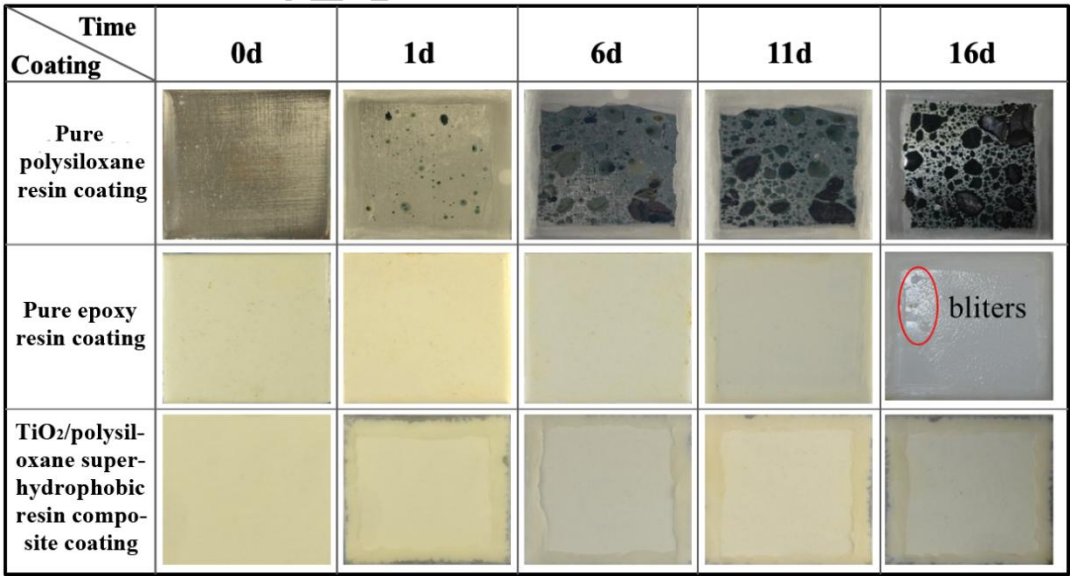

same immersion test compared with the other two coatings.

Figure 17. Corrosion morphology of polysiloxane resin coating, epoxy resin coating and super-hydrophobic TiO_2/polysiloxane resin composite coating immersed in 3.5 wt % NaCl

solution

Figure 18 shows the contact angles of the TiO_2/polysiloxane resin composite coatings after different immersion time. It can be seen that the contact angle decreases gradually with increasing immersion time. The composite coating, in fact, has lost its super-hydrophobicity after 16-day immersion test (the contact angle has reduced to 92° after 16-day immersion). However, the super-hydrophobicity of the composite coating reappears when the "old surface" (i.e., the surface exposed in the corrosion medium in the immersion test) was slightly polished. In this work, the composite coating after 16-day immersion test was half polished by sandpaper to remove the top surface layer which has lost the super-hydrophobicity. Figure 19 shows the wettability of "old surface" and "new surface" of the composite coating. It is seen that the "old surface" and "new surface" exhibit greatly different hydrophobicity. The hydrophobicity of the "new surface" is much better than the "old surface". The reappearance of the super-hydrophobicity of the composite coating can be attributed to the special coating design, i.e., the super-hydrophobic TiO_2 nanoparticles acting as the matrix are bonded by a small amount of polysiloxane resin. This coating system ensures the super-hydrophobicity of the coating in the full thickness of the composite coating, and makes the super-hydrophobicity reappear when the "new surface" comes out. Therefore, it could be proposed that even when the top surface of the coating loses the super-hydrophobicity the composite coating can still prevent the corrosion medium penetrating into the coating below and substrate. This is consistent with the corrosion morphology of the super-hydrophobic TiO_2/polysiloxane resin composite coating

shown in Figure 17.

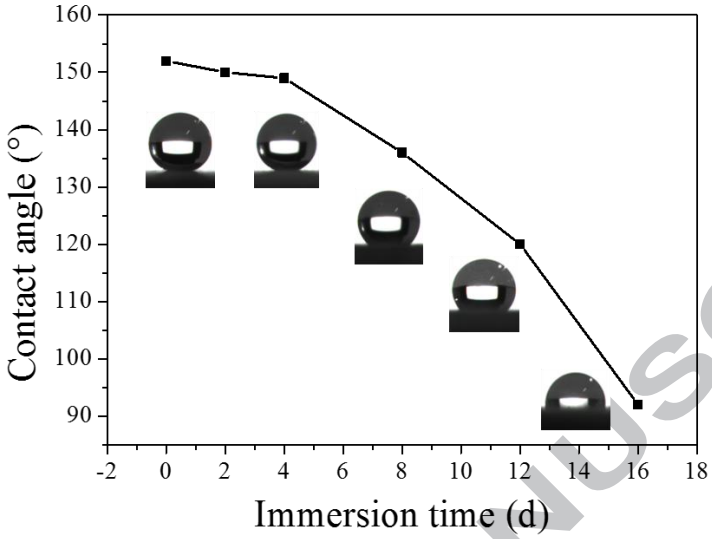

Figure 18. Water contact angles of the TiO_2/polysiloxane resin composite coating after different immersion time in 3.5 wt % NaCl solution

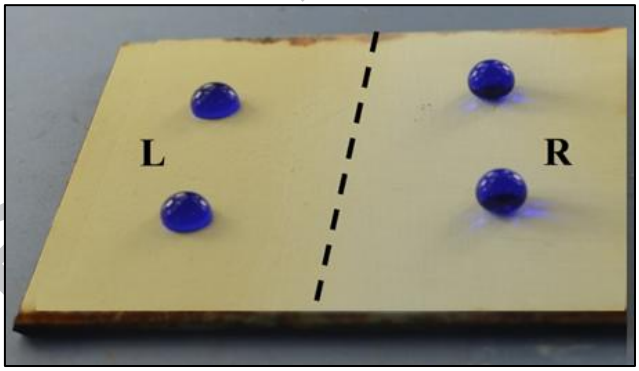

Figure 19. Wettability of the composite coating surface after 16-day immersion in 3.5 wt % NaCl solution (L: the old surface after immersion; R: the new surface after polishing with sandpaper)

4 Conclusions

In the present work, the rutile TiO_2 nanoparticles were firstly modified and found to possess excellent super-hydrophobicity and thermal stability. Then, a durable and robust super-hydrophobic TiO_2/polysiloxane resin composite coating was fabricated via a facile blending of modified TiO_2 nanoparticles and a polysiloxane resin. Based

on the characterization and properties testing results of modified TiO_2 nanoparticles and TiO_2/polysiloxane resin composite coating, we can draw the following conclusions:

- The modified TiO_2 nanoparticles showed a good hydrophobicity with a CA value of 151° and a SA value of close to 0°.
- The super-hydrophobic composite coating was obtained when the weight ratio of TiO_2 nanoparticles and polysiloxane resin was close to 2:1.
- The TiO_2/polysiloxane resin composite coating had a good thermal stability with a weight loss less than 1% when the exposure temperature was below160 °C.
- Due to the design of full-thickness super-hydrophobicity, the composite coating can keep its super-hydrophobicity even when the coating surface was worn in the abrasion test.
- The TiO_2/polysiloxane resin coating immersed in 3.5 wt % NaCl solution for 16 days still showed good corrosion resistance although the top surface of the composite coating has lost the super-hydrophobicity.

Acknowledgments

The authors acknowledge funding support from the National Natural Science Foundation of China (51201183 and 51501226), Shandong Provincial Natural Science Foundation, China (ZR2014EL003), the Applied Fundamental Research Foundation of Qingdao Independent Innovation Plan (15-9-1-46-jch and 16-5-1-90-jch), and Fundamental Research Funds for the Central Universities"(14CX02221A, 16CX05017A and 17CX05023).

References

[1] Y. Liu, K. Zhang, W. Yao, J. Liu, Z. Han, L. Ren, Bioinspired structured superhydrophobic and superoleophilic stainless steel mesh for efficient oil-water separation, Colloids and Surfaces A: Physicochemical and Engineering Aspects 500 (2016) 54-63.

[2] J. Yong, Y. Fang, F. Chen, J. Huo, Q. Yang, H. Bian, G. Du, X. Hou, Femtosecond laser ablated durable superhydrophobic PTFE films with micro-through-holes for oil/water separation: Separating oil from water and corrosive solutions, Applied Surface Science 389 (2016) 1148-1155.

[3] H. Zhang, J. Yang, B. Chen, C. Liu, M. Zhang, C. Li, Fabrication of superhydrophobic textured steel surface for anti-corrosion and tribological properties, Applied Surface Science 359 (2015) 905-910.

[4] S. Zheng, C. Li, Q. Fu, W. Hu, T. Xiang, Q. Wang, M. Du, X. Liu, Z. Chen, Development of stable superhydrophobic coatings on aluminum surface for corrosion-resistant, self-cleaning, and anti-icing applications, Materials & Design 93 (2016) 261-270.

[5] J.-D. Brassard, D.K. Sarkar, J. Perron, Studies of drag on the nanocomposite superhydrophobic surfaces, Applied Surface Science 324 (2015) 525-531.

[6] H. Tian, J. Zhang, E. Wang, Z. Yao, N. Jiang, Experimental investigation on drag reduction in turbulent boundary layer over superhydrophobic surface by TRPIV, Theoretical and Applied Mechanics Letters 5 (2015) 45-49.

[7] A. Matin, N. Merah, A. Ibrahim, Superhydrophobic and self-cleaning surfaces

prepared from a commercial silane using a single-step drop-coating method, Progress in Organic Coatings 99 (2016) 322-329.

[8] W.-H. Huang, C.-S. Lin, Robust superhydrophobic transparent coatings fabricated by a low-temperature sol–gel process, Applied Surface Science 305 (2014) 702-709.

[9] Q. Shang, Y. Zhou, Fabrication of transparent superhydrophobic porous silica coating for self-cleaning and anti-fogging, Ceramics International 42 (2016) 8706-8712.

[10] P. Peng, Q. Ke, G. Zhou, T. Tang, Fabrication of microcavity-array superhydrophobic surfaces using an improved template method, Journal of colloid and interface science 395 (2013) 326-328.

[11] T. Rezayi, M.H. Entezari, Achieving to a superhydrophobic glass with high transparency by a simple sol–gel-dip-coating method, Surface and Coatings Technology 276 (2015) 557-564.

[12] S. Rezaei, I. Manoucheri, R. Moradian, B. Pourabbas, One-step chemical vapor deposition and modification of silica nanoparticles at the lowest possible temperature and superhydrophobic surface fabrication, Chemical Engineering Journal 252 (2014) 11-16.

[13] Y. Huang, D.K. Sarkar, X.G. Chen, Superhydrophobic aluminum alloy surfaces prepared by chemical etching process and their corrosion resistance properties, Applied Surface Science 356 (2015) 1012-1024.

[14] Z. Yuan, H. Chen, J. Tang, X. Chen, D. Zhao, Z. Wang, Facile method to fabricate stable superhydrophobic polystyrene surface by adding ethanol, Surface and

Coatings Technology 201 (2007) 7138-7142.

[15] H. Wang, E. Chen, X. Jia, L. Liang, Q. Wang, Superhydrophobic coatings fabricated with polytetrafluoroethylene and SiO 2 nanoparticles by spraying process on carbon steel surfaces, Applied Surface Science 349 (2015) 724-732.

[16] N. Sharifi, M. Pugh, C. Moreau, A. Dolatabadi, Developing hydrophobic and superhydrophobic TiO 2 coatings by plasma spraying, Surface and Coatings Technology 289 (2016) 29-36.

[17] X. Chen, J. Yuan, J. Huang, K. Ren, Y. Liu, S. Lu, H. Li, Large-scale fabrication of superhydrophobic polyurethane/nano-Al 2 O 3 coatings by suspension flame spraying for anti-corrosion applications, Applied Surface Science 311 (2014) 864-869.

[18] Y. Huang, D.K. Sarkar, X.-G. Chen, Superhydrophobic nanostructured ZnO thin films on aluminum alloy substrates by electrophoretic deposition process, Applied Surface Science 327 (2015) 327-334.

[19] Y. Zheng, Y. He, Y. Qing, C. Hu, Q. Mo, Preparation of superhydrophobic coating using modified CaCO 3, Applied Surface Science 265 (2013) 532-536.

[20] K. Song, A. Gao, X. Cheng, K. Xie, Preparation of the superhydrophobic nano-hybrid membrane containing carbon nanotube based on chitosan and its antibacterial activity, Carbohydrate polymers 130 (2015) 381-387.

[21] Y. Qing, C. Yang, N. Yu, Y. Shang, Y. Sun, L. Wang, C. Liu, Superhydrophobic TiO 2/polyvinylidene fluoride composite surface with reversible wettability switching and corrosion resistance, Chemical Engineering Journal 290 (2016) 37-44.

[22] M. Hancer, H. Arkaz, A facile fabrication of superhydrophobic nanocomposite

coating with contact angles approaching the theoretical limit, Applied Surface Science 354 (2015) 342-346.

[23] H. Wang, J. Zhao, Y. Zhu, Y. Meng, Y. Zhu, The fabrication, nano/micro-structure, heat-and wear-resistance of the superhydrophobic PPS/PTFE composite coatings, Journal of colloid and interface science 402 (2013) 253-258.

[24] Y. Lu, S. Sathasivam, J. Song, C.R. Crick, C.J. Carmalt, I.P. Parkin, Robust self-cleaning surfaces that function when exposed to either air or oil, Science 347 (2015) 1132-1135.

[25] B. Chen, J. Qiu, E. Sakai, N. Kanazawa, R. Liang, H. Feng, Robust and superhydrophobic surface modification by a "Paint+ Adhesive" method: applications in self-cleaning after oil contamination and oil–water separation, ACS applied materials & interfaces 8 (2016) 17659-17667.

[26] F. Zhang, Z. Shi, L. Chen, Y. Jiang, C. Xu, Z. Wu, Y. Wang, C. Peng, Porous superhydrophobic and superoleophilic surfaces prepared by template assisted chemical vapor deposition, Surface and Coatings Technology 315 (2017) 385-390.

[27] H. Tavana, C. Lam, K. Grundke, P. Friedel, D. Kwok, M. Hair, A. Neumann, Contact angle measurements with liquids consisting of bulky molecules, Journal of colloid and interface science 279 (2004) 493-502.

Research highlights

1. Polysiloxane resin was used in the fabrication of superhydrophobic coating.
2. The nano-TiO_2 were used as the body of composite coating.
3. The polysiloxane resin was used as the binder bond the nanoparticles together.
4. The coating can maintain super-hydrophobicity even the coating surface was worn.